Comptes rendus - Geoscience 351 (2019) 384–394

Contents lists available at ScienceDirect

Comptes rendus - Geoscience

www.journals.elsevier.com/comptes-rendus-geoscience

Tectonics, Tectonophysics

Tectono-metamorphic evolution of the European continental margin involved in the Alpine subduction: New insights from Alpine Corsica, France

Maria Di Rosa [a, b, *], Chiara Frassi [a], Francesca Meneghini [a], Michele Marroni [a, c], Luca Pandolfi [a, c], Alberto De Giorgi [a]

[a] Dipartimento di Scienze della Terra, Università di Pisa, Pisa, Italy
[b] Dipartimento di Scienze della Terra, Università di Firenze, Firenze, Italy
[c] Istituto di Geoscienze e Georisorse, IGG-CNR, Pisa, Italy

ARTICLE INFO

Article history:
Received 25 July 2018
Accepted 1 December 2018
Available online 12 March 2019
Handled by Isabelle Manighetti

Keywords:
Continental subduction
Polyphase exhumation
P–T–d paths
HP metamorphism
Alpine Corsica

ABSTRACT

In Corsica, continental units (the Lower Units) affected by high-pressure metamorphism represent the remains of the European margin deformed during the Alpine orogeny. In order to document how Alpine deformation and metamorphism changed along the European margin involved in the Alpine subduction, we selected three key areas: the Corte, Cima Pedani, and Ghisoni transects. The three transects show a broadly similar lithostratigraphy. They are characterized by a Variscan basement intruded by Permo-Carboniferous metagranitoids, and by a sedimentary cover including Mesozoic carbonates and middle to late Eocene breccias and sandstones. The three transects recorded a similar deformation history with three deformation phases. Thermo-baric estimations, instead, reveal that each unit was exhumed along an independent retrograde path within the orogenic Alpine wedge. In particular, the lowest units of the Lower Units stack were exhumed along an isothermal path, whereas those located at upper structural levels experienced progressive heating.

1. Introduction

The exposure at the Earth's surface of continental units affected by (ultra-)high-pressure (U)HP metamorphism indicates that the continental crust can move along the plates interface reaching depths greater than 50 km (Guillot et al., 2009 and references therein). The preservation of these units testifies to the crucial role played by subduction processes in the growing and recycling of the continental crust and help solve fascinating and challenging problems, such as the understanding of the tectonic processes responsible for the subduction and subsequent exhumation of granitic and metasedimentary rocks.

Alpine Corsica, cropping out in the northeastern sector of island of Corsica, is a key area for studying continental-derived units affected by HP metamorphic conditions. Alpine Corsica is made of continental- and oceanic-affinity units, derived from the thinned European margin and the Western Tethys Ocean (Durand-Delga, 1984; Frizon de Lamotte et al., 2011; Lacombe and Jolivet, 2005; Malasoma et al., 2006; Molli et al., 2006), buried during the Eocene subduction of the European margin and subsequently affected by syn-convergent exhumation (Brunet et al., 2000; Gueydan et al., 2017; Malasoma and Marroni, 2007; Molli and Malavieille, 2011; Rossetti et al., 2015;

* Corresponding author. Dipartimento di Scienze della Terra, Università di Pisa, Via Santa Maria, 53, 56126 Pisa, Italy.
E-mail address: maria.dirosa@unifi.it (M. Di Rosa).

https://doi.org/10.1016/j.crte.2018.12.002
1631-0713/

Vitale Brovarone and Herwartz, 2013 and references therein).

To constrain the processes responsible for continental crustal recycling and exhumation of HP rocks and to understand how (and if) these processes change along the continental margin, we compared tectono-metamorphic and stratigraphic data from three transects across the western border of the Corsica Alpine tectonic prism, i.e. from north to south (Fig. 1), the Cima Pedani, Corte, and Ghisoni transects.

2. Geological setting

The island of Corsica is a piece of continental lithosphere isolated between two Tertiary back-arc basins: the Liguro-Provençal basin, to the west, and the Tyrrhenian basin, to the east. The island exposes two geological domains separated by NNW–SSE-trending tectonic boundary (e.g., Durand-Delga, 1984): the Alpine and the Hercynian Corsica domains. Although locally obliterated by the late Eocene–early Oligocene sinistral strike-slip fault zone (Maluski et al., 1973), known as the Central Corsica Shear Zone (CCSZ; Waters, 1990), this tectonic boundary ideally marks the thrust zone of Alpine Corsica onto the Hercynian Corsica Domain (Fig. 1).

The latter domain, which is widely exposed in the Southwest of the islands of Corsica and Sardinia, represents the southern Variscan realm (Matte, 2001). It consists of Pan-African and Variscan metamorphic rocks (Rossi et al., 2009) intruded by Permo-Carboniferous magmatic rocks. The Permo-Mesozoic covers are represented by Permian rhyolites, by volcanic and volcanoclastic and sedimentary deposits (conglomerates, arenites and pelites, Rossi et al., 2009), and by Mesozoic carbonates, unconformably topped by middle to late Eocene deposits (Durand-Delga, 1984).

Alpine Corsica is exposed in the northeastern part of the island. In analogy to the Western Alps, it consists of a stack of units derived from the Ligure-Piemontese oceanic basin and the neighbouring Adria and Europe continental margins (Durand-Delga, 1984; Maggi et al., 2014; Marroni and Pandolfi, 2007; Marroni et al., 2017; Molli and Malavieille, 2011; Saccani et al., 2015). These units are metamorphosed and deformed during the Late Cretaceous (?)–late Eocene eastward-dipping subduction of the Ligure-Piemontese oceanic lithosphere and of the European margin. This process was succeeded by the west-dipping subduction of the Adria margin and the incipient continental collision (Malavieille et al., 1998; Marroni et al., 2004, 2017; Molli and Malavieille, 2011; Vitale Brovarone and Herwartz, 2013). In the early Oligocene, the convergence-related processes were replaced by large-scale extension related to the Adria slab south-westward retreat that induced the collapse of the thickened orogenic wedge, as well as the opening of the Liguro-Provençal basin and then of the Tyrrhenian (Brunet et al., 2000; Gueydan et al., 2017).

The present-day tectonic setting of the Alpine Corsica Domain consists of a stack of three groups of tectonic units known as, from top to bottom, the Upper Units, the "Schistes lustrés" Complex and the Lower Units (Durand-Delga, 1984; Malavieille et al., 1998; Molli and Malavieille, 2011; Pandolfi et al., 2016). The Miocene (Burdigalian–Langhian) deposits of the Saint-Florent and Francardo basins (Cavazza et al., 2001, 2007; Ferrandini et al., 2003) seal their reciprocal contacts.

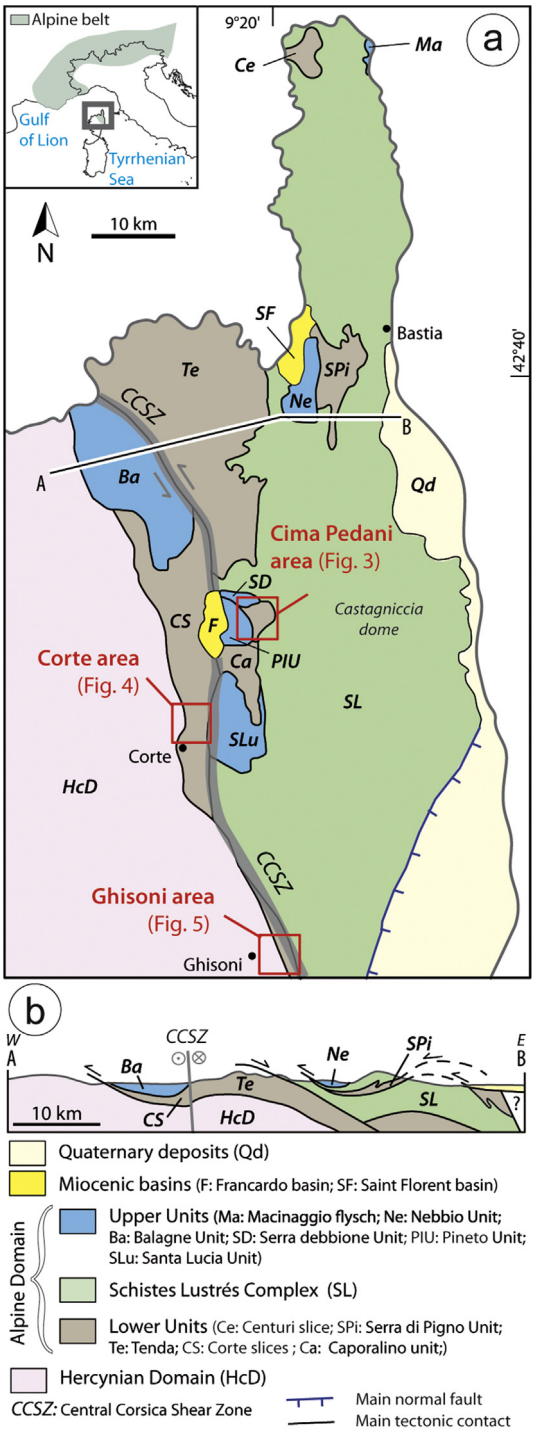

Fig. 1. (a) Tectonic sketch of Alpine Corsica; the location of the three studied areas (i.e. Figs. 3–5) is indicated. (b) Schematic cross-section of the island of Corsica (modified after Malavieille et al., 1998).

The very low-grade metamorphic Upper Units (i.e. "Nappes supérieures" of Durand-Delga, 1984), include Middle to Late Cretaceous ophiolitic units associated with slices of Late Cretaceous carbonate turbidites (Pandolfi et al., 2016 and references therein). The "Schistes lustrés" Complex consists of ophiolitic and oceanic-continental transitional sequences deformed under eclogite to blueschists facies conditions during the Late Cretaceous (?) to late Eocene subduction (Gueydan et al., 2017; Vitale Brovarone and Herwatz, 2013 and references therein). The Lower Units represent fragments of the European margin affected by late Eocene HP–LT metamorphism acquired during their subduction below the Adria margin (Bezert and Caby, 1988; Di Rosa et al., 2017a, b; Faure and Malavieille, 1981; Malasoma and Marroni, 2007; Mattauer et al., 1981; Molli and Malavieille, 2011).

The stack was lately affected by the brittle deformations related to the CCSZ (Di Rosa et al., 2017a; Lacombe and Jolivet, 2005), and during the early Miocene time, Alpine Corsica underwent a generalized extension (Cavazza et al., 2001; Danisik et al., 2007) leading to the development of basins, like those of Francardo and Saint-Florent (Fig. 1). The ramp-flat geometry of the normal faults is responsible for large-scale rollover anticlines and synclines, probably like that documented in the Castagniccia dome (Gueydan et al., 2017).

3. Methods

The 1:50,000 scale geological maps published by BRGM, France (Rossi et al., 1994, 2012) were used as a first cartographic base for the geology of the Cima Pedani, Corte, and Ghisoni regions, objects of this study (see the Corte and Bastelica sheets of the BRGM maps database). Detailed geologic mapping (scale 1:5000) was achieved during our work in the three areas, coupled with mesoscopic structural analyses that were conducted in the three areas. Detailed microstructural investigations were performed on metapelites and on Late Variscan metagranitoids. *P–T* conditions were estimated using the chlorite-phengite multi-equilibrium thermodynamic technique (Vidal and Parra, 2000) for each tectonic unit. The Electron probe microanalysis analyses were acquired on the JEOL JXA apparatus of the IsTerre (Grenoble, France) equipped with five wavelength-dispersive spectrometers and treated with XMapTools 2.1.3 (Lanari et al., 2014) and ChlMicaEqui softwares. We estimated the *P* and *T* conditions for phengite–chlorite pairs grown in different microstructural domains, elaborating pressure–temperature–deformation paths for each tectonic unit. To corroborate our results, we also used classical geobarometer and geothermometers (see Supplementary Material).

4. Tectono-metamorphism and stratigraphy of the Lower Units in the Cima Pedani, Corte and Ghisoni areas

4.1. Tectono-stratigraphy

The Lower Units consist of Variscan metamorphic rocks (i.e. Roches Brunes Fm.) and Permo-Carboniferous magmatic and volcanics products (metagranitoids and Metavolcanic and Metavolcaniclastic Fm., Fig. 2). The post-Paleozoic sequence consists of Mesozoic platform-type metacarbonates and middle to late Eocene metasandstones and metabreccias, unconformably lying on both the Variscan basement and the Permo-Mesozoic sequence (Fig. 2).

4.1.1. Cima Pedani area

In the Cima Pedani area, the Lower Units (Canavaggia Unit – CAU, Pedani Unit – PEU and Scoltola Unit – SCU) crop out in a tectonic window delimited by the "Schistes lustrés" Complex (i.e. Lento Unit – LEU) and the Upper Units (i.e. Serra Debbione Unit – SDU and Pineto Unit – PIU) (Figs. 3 and 6).

CAU is made of metagranitoids intruded in the "Roches brunes" Fm., covered by the Permian metavolcanics and metavolcaniclastics, in turn unconformably covered by the Metabreccia and Metasandstone Fms. (Fig. 2, Puccinelli et al., 2012). The Mesozoic sequence is missing in CAU, whereas in PEU, it is well represented at the top of the Permian Metavolcanic and Metavolcaniclastic Fm. (Fig. 2). SCU is represented exclusively by the Metasandstone and Metabreccia Fms..

4.1.2. Corte area

In the Corte area (Figs. 1, 4 and 6; Di Rosa et al., 2017a, 2017b; Rossi et al., 1994), the Lower Units (i.e. the "Écailles

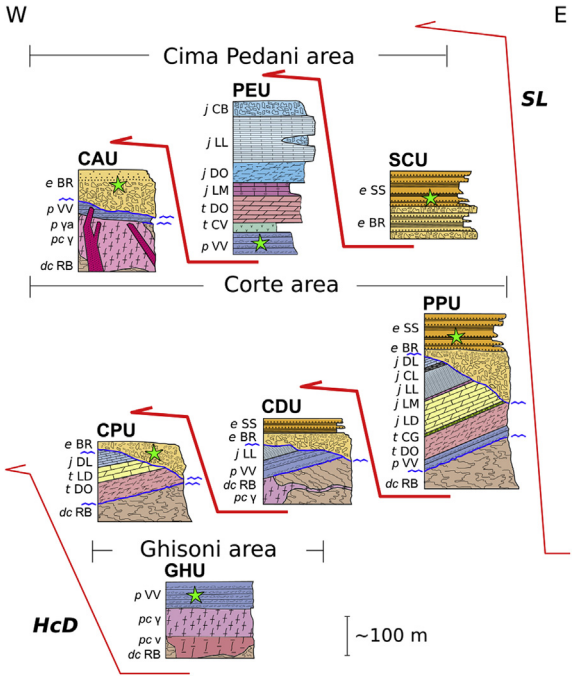

Fig. 2. Stratigraphic logs of the Lower Units in the Cima Pedani, Corte, and Ghisoni areas (the green star indicates the metapelitic lithotype sampled and used for the study of the metamorphism). dc RB: "Roches brunes" Fm.; pc γ: metagranitoids; pc ν: epidote-bearing metagabbros; pc γa: dykes complex; p VV: Metavolcanic and Metavolcaniclastic Fm.; t CV: Cavernoso Metalimestone Fm.; t DO: Lower Metadolostone Fm.; t CG: Metaconglomerate Fm.; t LD: Metalimestone and Metadolostone Fm.; j LM: Lumachella Metalimestone Fm.; j DO: Upper Metadolostone Fm.; j LL: Laminated Metalimestone Fm.; j CB: Metacarbonate breccia; j CL: Cherty Metalimestone Fm.; j DL: Detritic Metalimestone Fm.; e BR: Metabreccia Fm. and e SS: Metasandstone Fm.

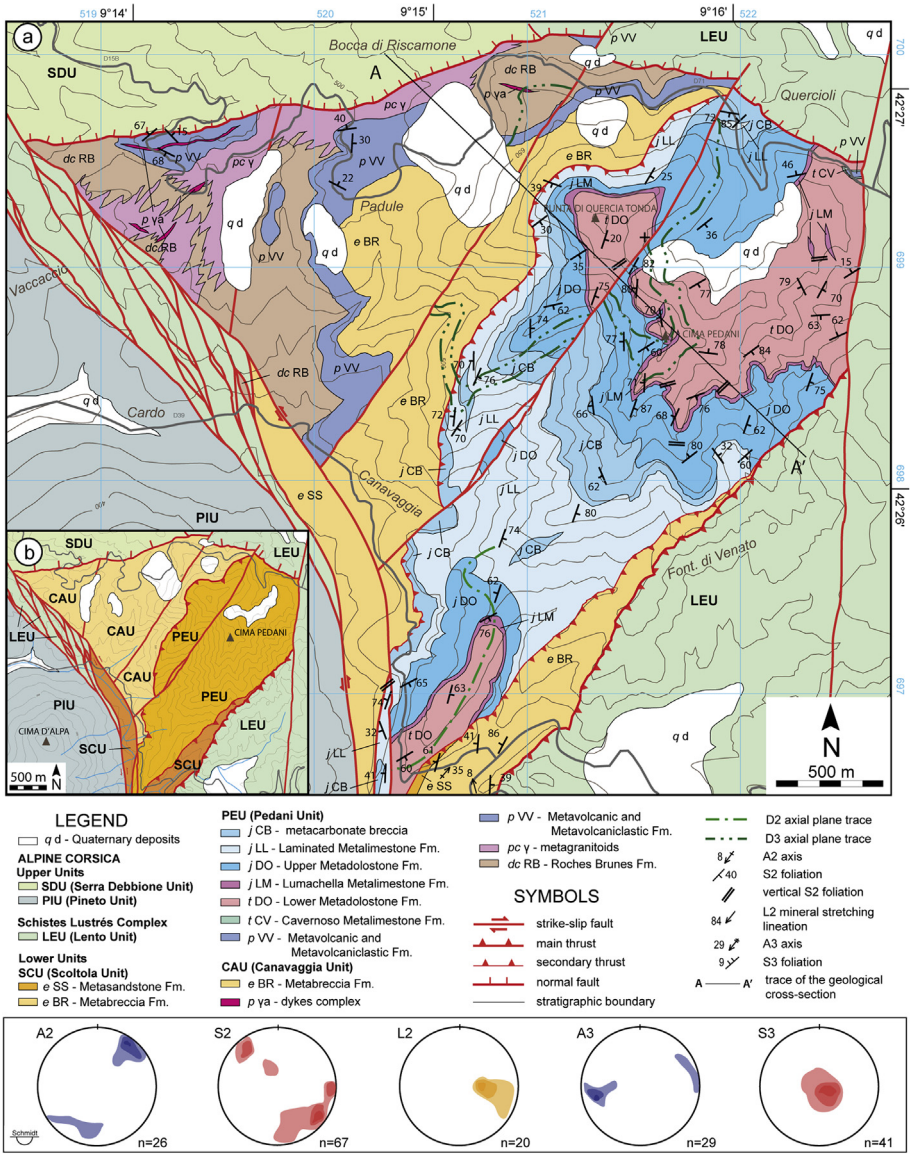

Fig. 3. (a) Geological map and stereographic projections of the main structural elements documented in the Cima Pedani area. (b) Tectonic sketch of the area.

de Corte": Castiglione-Popolasca Unit – CPU, Croce d'Arbitro Unit – CDU and Piedigriggio–Prato Unit – PPU) are sandwiched between the Hercynian Corsica Domain and the "Schistes lustrés" Complex (i.e. Inzecca Unit - IZU). CPU is made of Mesozoic dolostones to limestones lying above the "Roches brunes" Fm. and unconformably covered by the Metabreccia and Metasandstone Fms. (Fig. 2). In CDU, the Variscan basement is topped by the Permian Metavolcanic and Metavolcaniclastic Fm. and by the Mesozoic sequence (i.e. Laminated Metalimestones Fm.). The Metabreccia and the Metasandstone Fms. overlie unconformably both the Paleozoic and Mesozoic Fms. PPU has the more complete succession (Fig. 2). It consists of the Roche Brunes Fm., the Permian Metavolcanic and Metavolcaniclastic Fm., a complete Mesozoic succession and the Metabreccia and Metasandstone Fms. Moreover, the middle Eocene angular unconformity crosscuts the Mesozoic sequence down to the Norian Metadolostone Fm. (Fig. 2).

4.1.3. *Ghisoni area*

In the Ghisoni area (Figs. 1 and 5; Garfagnoli et al., 2009), the Lower Units are sandwiched between the Hercynian Corsica Domain and the "Schistes lustrés" Complex (i.e. Inzecca Unit – IZU) and are strongly overprinted by the CCSZ (Fig. 6). They are represented by the Ghisoni Unit (GHU), which consists, from bottom to top, by the Roches Brunes Fm., the epidote-bearing metagabbros (emplaced within the continental crust during the oldest Permo-Carboniferous intrusive pulse), the Late Paleozoic metagranitoids, and the Permian Metavolcanic and Metavolcanoclastic Fm. (Fig. 2).

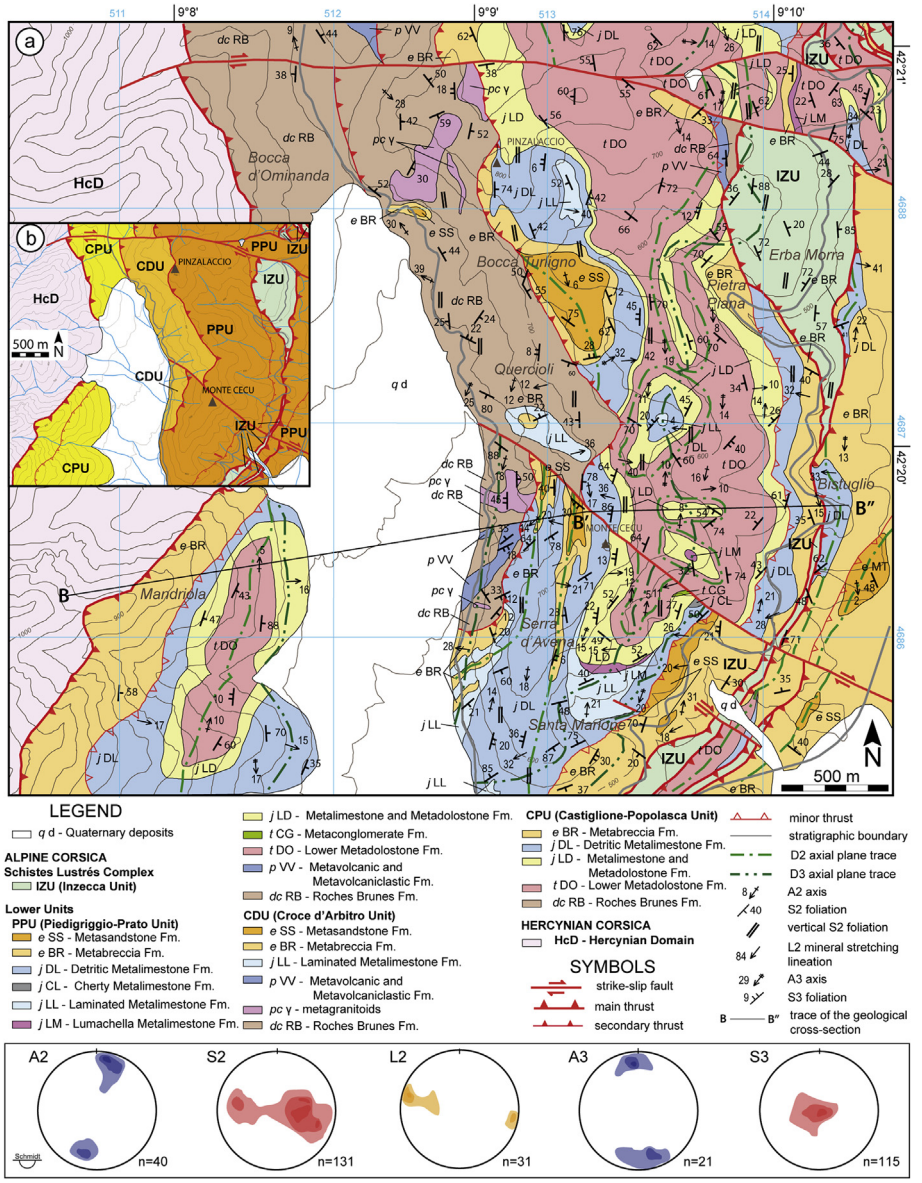

Fig. 4. Geological map and stereographic projections of the main structural elements documented in the Corte area. (b) Tectonic sketch of the area. Modified after Di Rosa et al. (2017a; 2017b).

4.2. Structural analysis

In the studied transects, the Lower Units recorded a similar deformation history, with three deformation phases (D1–D3) described in the following sub-sections. The microscopic description of foliations was performed taking as a reference the Permian Metavolcanic and Metavolcaniclastic Fm. and the metapelitic layers in the Eocene Metabreccia and Metasandstone Fms., where the *P–T* paths were calculated, whereas quartz microstructures were investigated in the Permo-Carboniferous metagranitoids.

In the field, the pervasive foliation documented in the metagranitoids is parallel to the main foliation documented in the post-Variscan covers (i.e. the S2 foliation). As a consequence, we described the meso- and microscopic feature of the metagranitoids foliation within the D2 phase section.

Considering the goal of this paper, the presentation of data and their discussion will be focused on the three deformation phases documented in the field. Post-D3 tectonics is not described and discussed.

4.2.1. D1 phase

The structural elements produced during the oldest deformation phase (D1) are rarely observable at the mesoscale. They are represented by F1 sheath folds in Laminated Metalimestone Fm. and by an S1 foliation

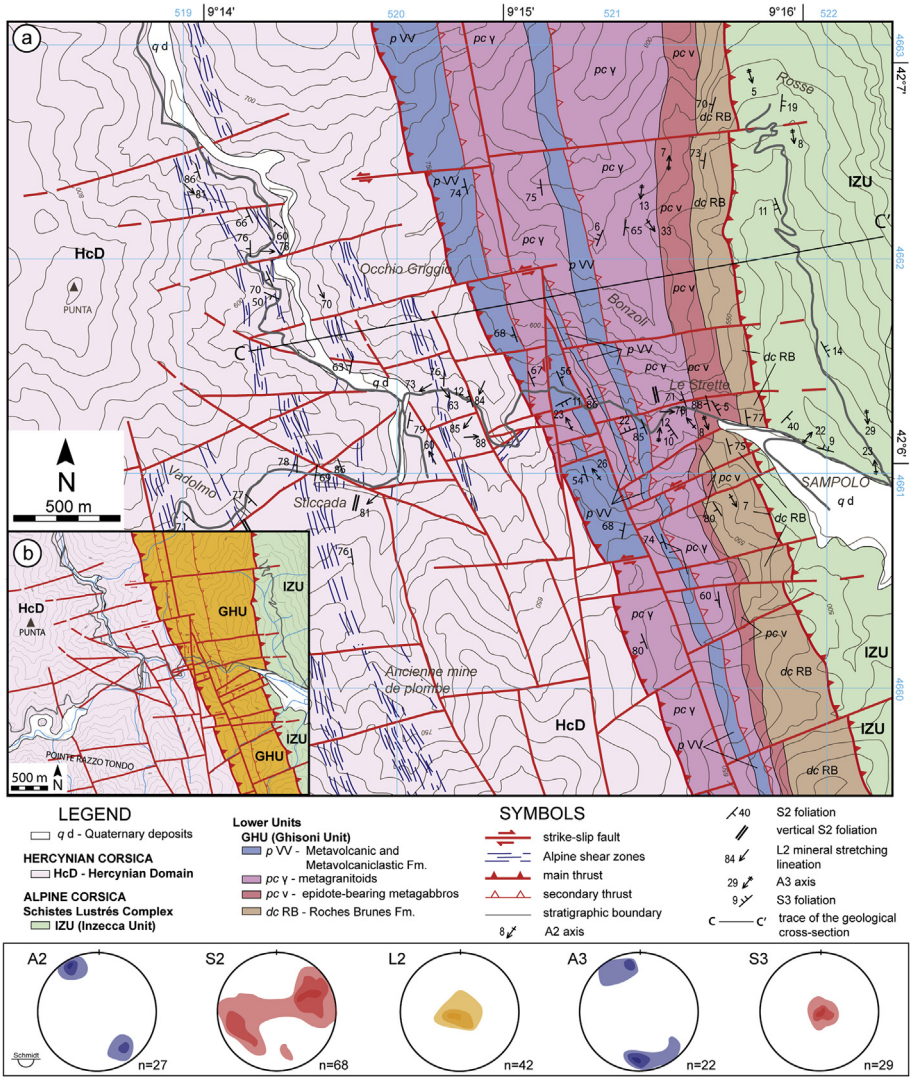

Fig. 5. (a) Geological map and stereographic projections of the main structural elements documented in the Ghisoni area. (b) Tectonic sketch of the area.

preserved in the hinge zones of the F2 folds (Fig. Sm1a and b). At the microscopic scale, S1 foliation is often preserved within D2 microlithons as a continuous, coarse-grained schistosity marked by the syn-kinematic growth of chlorite, phengite, albite, quartz, and calcite (Sm1b). No relics of an earlier foliation were documented within the D2 microlithons in the metagranitoids.

4.2.2. D2 phase

The D2 phase is responsible for the main structural elements documented at the mesoscale (Sm1). This phase produced F2 isoclinal and similar folds associated with a S2 axial plane foliation, and also top-to-the-west shear zones, located within the units or close to the tectonic contacts between them. The trend of the A2 axes ranges from NE–SW in the Cima Pedani area (Fig. 3), to NNE-SSW in the Corte area (Fig. 4), and to SE–NW in the Ghisoni area (Fig. 5), always plunging less than 30° either toward north or south. Together with the A2 trending axes, the S2 axial planar foliation changes from NE–SW in the Cima Pedani area, to NNE–SSW in the Corte area, and to NNW–SSE in the Ghisoni area, showing dips either to the west or the east probably as a result of later D3 folding. The S2 foliation bears mineral and stretching L2 lineations that generally show a rough east-west trend with variable plunge. Along the limbs of the F2 folds, the S2 foliation is classified as a continuous foliation, whereas in the hinge zone of F2 folds, it can be classified as a gradational to discrete spaced crenulation cleavage.

The S2 foliation represents the main structural element documented at the microscopic scale (Sm1b, d). In metapelites, it is marked by recrystallized albite, quartz, calcite, chlorite, and phengite. Within the D2 shear zone, metamorphic phyllosilicates fill asymmetric tails of σ- and δ-type porphyroclasts (Passchier and Trouw, 2005) of quartz and feldspar pointing to a top-to-the-west sense of shear. Additional kinematic indicators are S–C/C′ fabrics, mica fishes, and bookshelf structures in feldspar.

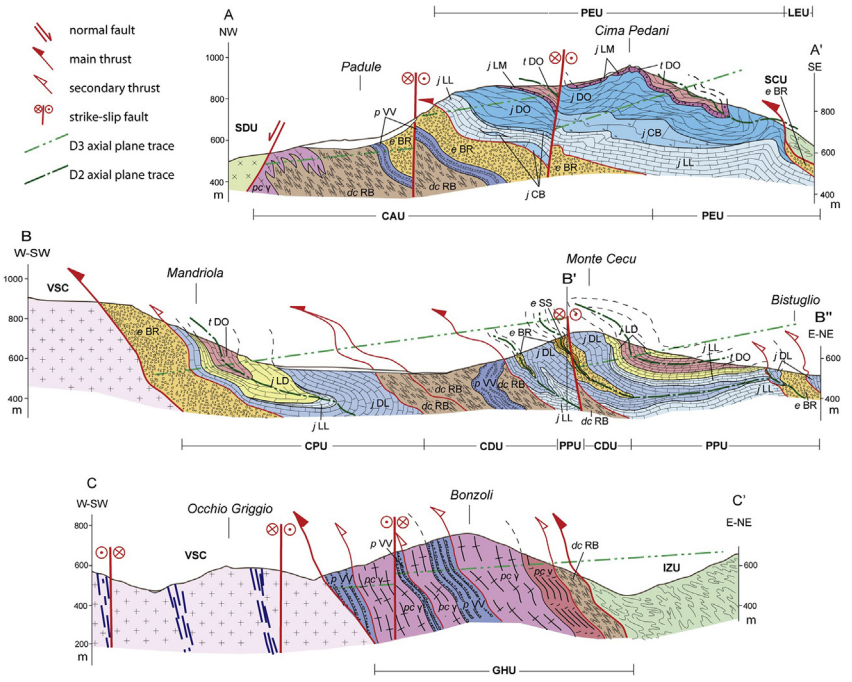

Fig. 6. Geological cross-sections of the (a) Cima Pedani, (b) Corte (modified after Di Rosa et al., 2017a, 2017b), and (c) Ghisoni areas. See Figs. 3–5 respectively, for locations.

Metagranitoid samples from CAU (Cima Pedani), CPU (Corte area), and GHU (Ghisoni area) have the same protoliths consisting of quartz + k-feldspar + plagioclase + white micas (±biotite). They show poorly developed protomylonitic fabrics in CAU and protomylonitic to ultramylonitic fabrics (Passchier and Trouw, 2005) in CPU and in GHU. Discontinuous layers of recrystallized white mica (up to 100 μm) ± biotite, and granoblastic layers of fine-grained recrystallized quartz ± plagioclase (albite) mark the mylonitic foliation. It generally wraps centimeter-sized feldspars and quartz grains, aggregates of quartz + feldspar, and lenses of very fine-grained (less than 6 μm) recrystallized quartz and feldspar. In CPU, feldspar and quartz grains show nearly sub-euhedral geometry, whereas in CAU they are weakly elongated, with the main axis parallel to the mylonitic foliation. The strongest aspect ratio (R_{XZ}) and parallelism are observed in GHU, where quartz and feldspar reached $R_{XZ\ max} = 13{:}3$ and 9:3, respectively.

In CAU, quartz and feldspar crystals often show angular shape and reduction in grain size produced by microcracking and microfaulting, indicative of a late-to post-foliation cataclastic event. Calcite crystals filling syntectonic veins, show type-IV deformation twins (Ferrill et al., 2004), indicative of deformation temperatures greater than 250 °C.

In GHU and CPU, centimeter-sized quartz crystals are affected by undulatory extinction, deformation lamellae, deformation bands (developing frequently as conjugate sets), and bulging (e.g., Passchier and Trouw, 2005). The biggest crystals show conjugate bands of recrystallized grains (4–8 μm) oriented at low and high angle with respect to the mylonitic foliation. The crystal preferred orientation, determined with a lambda plate inserted in an optical microscope, is weak, and the preferred orientation of grain shape is limited to the asymmetric tails in σ-porphyroclasts. Locally, quartz crystals are strongly elongated and partly recrystallized, indicating that incipient subgrain rotation recrystallization mechanisms occurred. Rare deformation twins are also present. These microstructures indicate that dislocation creep represents the main deformation mechanism in quartz during the development of the main foliation, suggesting a deformation temperature of ~400 °C. Feldspar shows features typical of low-temperatures conditions (<400 °C) such as undulatory extension, microfaulting, and boudinage. S–C′ fabric, σ-type porphyroclasts of feldspar showing asymmetric tails of recrystallized quartz and/or white micas, and bookshelf structures in feldspar represent the main kinematic indicators pointing top-to-the-west in both GHU and CPU.

4.2.3. D3 phase

The D3 phase produced open-to-close gently inclined F3 folds associated with a spaced and sub-horizontal S3 axial plane foliation (Sm1c). The A3 axes trend changes in the studied transects from ENE–WSW in the Cima Pedani area to NNE-SSW in the Corte and Ghisoni areas. At the mesoscopic scale, F3 folds affected both the tectonic contacts within the Lower Units and those separating the Lower Units from the “Schistes lustrés” Complex and the Upper Units (Fig. 6). At the microscopic scale, the S3 foliation can be classified as spaced crenulation cleavage associated with minor metamorphic recrystallizations of calcite, Fe-oxides and quartz. In the metagranitoids, the D3 phase was documented exclusively in the thicker phyllosilicate-rich-layers as symmetric microfolds (Sm1d).

4.3. P–T equilibrium conditions

4.3.1. Chlorites and phengites characterization

The chlorite (Chl) and phengite (Phg) end-members proportions in the analysed micro-areas of the samples are reported in Supplementary Material (Table Sm1). The Chl of all the samples studied are characterized by a composition similar to the pure clinochlore (Cl) and daphnite (Da) end-members (>60%). Chl in CAU, PEU and SCU show a higher amesite (Am) content with respect to the other units, suggesting that they have reached higher temperature conditions (Vidal et al., 2001). In all the studied samples, Phg composition is intermediate between celadonite (Ce) and muscovite (Mu) end-members, with a pyrophyllite (Py) content always lower than 35%, suggesting high-*P* conditions (Vidal and Parra, 2000). The composition of the Phg grown along the S1 foliation ranges between the Ce and Mu end-members from 40–60% to 30–60%, respectively, whereas those grown along the S2 foliation are characterized by an increasing Py content observable in all the units. Inside this general trend, several small-scale differences in the proportions of the end-members can be recognized.

4.3.2. Multi-stepped P–T paths

The Chl–Phg–quartz–water multiequilibrium method (Vidal and Parra, 2000) allows us to calculate the *P–T* equilibrium condition for each selected couple of Chl–Phg (according to Vidal and Parra (2000), the admitted error for *P* and *T* calculated with this method is 0.2 GPa and 30 °C, respectively). In all the analysed samples, we measured different equilibrium conditions from different Chl–Phg couples in order to determine: (1) the baric (P_{max}) peak, (2) the thermic (T_{max}) peak, and (3) the lower *P–T* conditions of recrystallization. The P_{max} and T_{max} conditions are obtained from two different generations of Chl and Phg grown along the S1 foliation, whereas the couples of Chl and Phg in equilibrium at lower *P–T* conditions have grown along the S2 foliation.

Although the three equilibrium conditions have been observed in all samples, the absolute *P* and *T* estimates in each sample vary in a range of 0.3 GPa and 100 °C (See Supplementary Material, Table Sm2). The *P–T–d* (pressure–temperature–deformation) paths obtained for each unit show two different trends: a straight path (GHU and CPU) and a more complicated trend (PPU, SCU, CAU and PEU) (Fig. 7). In GHU, the two generations of chlorite and phengite associated with the S1 foliation are in equilibrium at $P = 0.81–0.72$ GPa and $T = 245–250$ °C and at $P = 0.68–0.39$ GPa and $T = 263–243$ °C, respectively. In CPU, the first generation is in equilibrium at $P = 1.22–1.10$ GPa and $T = 250–330$ °C, whereas the second is in equilibrium at $P = 0.82–0.56$ GPa and $T = 320–350$ °C (Fig. 7) (Di Rosa et al., 2017a). The rest of the units are characterized by variable *P–T* conditions related to the *P*-peak and a subsequent reverse trend of increasing *T* and decreasing *P*. The differences between the samples in the *P–T* conditions related to the *T*-peak are smaller than those of the *P*-peak. The evolution from the second generation (i.e. *T*-peak) and the third generation (i.e. related to the S2 foliation) of Chl–Phg couples is associated with an abrupt cooling of ca. 100 °C.

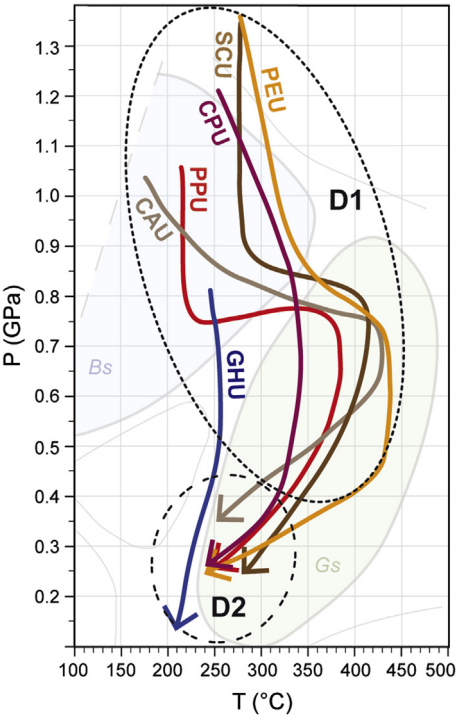

Fig. 7. Summary of the pressure–temperature–deformation (*P–T–d*) paths of the Lower Units in the three selected areas. *P–T–d* paths of CPU and PPU are after Di Rosa et al. (2017a). The stacking of the Lower Units occurred during the late D2 phase. Bs: blueschist facies; Gs: greenschist facies.

5. Discussion

5.1. Stratigraphy

Differently from the classification of lithotypes by Amaudric du Chaffaut et al. (1983), who defined a different stratigraphy in each study area, we propose a unique stratigraphic evolution during the Permian–late Eocene time span along the European margin. Minor differences within the units are mainly due to (Fig. 2): (1) the presence/lack of the Variscan basement and of the Permian sediments, (2) the presence/lack of the Mesozoic sequence, (3) if present, the thickness of the Mesozoic sequence, (4) if present, the thickness of the middle to late Eocene sequence and the position of the angular unconformity at its base.

As postulated by Durand-Delga (1984), the entire European continental margin is characterized by two main sedimentary cycles divided by a regional angular unconformity: the Variscan cycle and the Alpine cycle. The former consists of Devonian to Early Carboniferous low-to-medium grade metamorphic rocks (i.e. the Roches Brunes Fm. *Auctt*). The Alpine cycle is characterized by two stratigraphic sequences, separated by an angular unconformity located at the base of middle Eocene. The older sequence starts with the intrusion of the Permo-Carboniferous monzogranites and the deposition of Permian volcanics and volcaniclastic sediments (Metavolcanic and Metavolcaniclastic Fm.) and continues with the deposition of

Jurassic–Triassic carbonate sequences. The younger alpine cycle is instead represented by the Eocene foredeep sequence (i.e. Metabreccia and Metasandstone Fms.) crosscutting not only the carbonates of the first cycle, but also the Variscan sequence (Fig. 2).

As documented in the Alps (e.g., Michard and Martinotti, 2002), subduction-related peripheral bulge can produce or enhance local uplift with consequent erosion of the forebulge and the deposition of unconformable foredeep sequences. In our reconstruction, the same processes may have occurred when the European plate reached the Eocene subduction zone. The angular unconformity documented inside the Alpine cycle (i.e. separating the Paleozoic–Mesozoic passive margin from the middle to late Eocene foredeep deposits) in all the studied Lower Units represents a regional surface produced by erosion processes affecting the continental lithosphere during its approach toward the subduction zone.

5.2. The Lower Units from subduction to exhumation: the D1 and D2 phases

The Lower Units exposed in the Cima Pedani, Corte and Ghisoni areas share the same deformation history, but record different *P–T* exhumation paths (Fig. 7). The main ductile event preserved in all the units is the D2 phase. It is a non-coaxial deformation phase characterized by isoclinal folds, penetrative S2 foliation and top-to-the west shear zones (i.e. top-to-the foreland shearing, considering the eastward-dipping subduction plane reconstructed for the Alpine evolution of this sector of Corsica). Relics of the earlier D1 deformation phase are scarce and preserved in D2 low-strain domains.

The thermo-baric estimates obtained by chlorite-phengite pairs grown during the D1 and D2 phases in the Lower Units exposed in the Ghisoni area constrain only the retrograde path recorded in the Lower Units during their exhumation up to shallower levels along the base of the Alpine Corsica wedge, today represented by the "Schistes lustrés" Complex. No prograde path related to the underthrusting of the unit and to their transfer at the base of the Alpine Corsica wedge is recorded. These results corroborate those documented in Corte (Di Rosa et al., 2017a).

In detail, three generations of phyllosilicates were documented in the Ghisoni samples. The growth of the first two, documented along the relics of S1 foliation, occurred during pressure, then temperature peak conditions, respectively. This implies that the D1 phase occurred from HP–LT to LP–HT metamorphic conditions (Fig. 7). A third generation of Chl and Phg have grown along the S2 foliation and are in equilibrium at lower *P* and *T* conditions. Even if the three generations of Chl–Phg pairs have been documented in all the units, the *P–T* conditions at which they were in equilibrium differ, suggesting that each unit followed an independent trajectory of exhumation until the end of the D2 phase.

The straight path documented in GHU and CPU indicates that their exhumation during the D1 and D2 phases occurred under almost isothermal paths. GHU shows a maximum change in temperature during the D1 phase between P_{peak} and T_{peak} of less than 20 °C, and between the D1 phase T_{peak} and the D2 phase of ca. 60 °C (Fig. 7). This trend indicates that the GHU stationed shortly in the deepest position and was quickly exhumed; assuming an average crustal geobaric gradient of 30 MPa/km (Best, 2003), it is estimated that GHU moved from ca. 27 to ca. 4 km. CPU recorded greater differences in pressure and temperature during the D1 phase and between D1 and D2 phase (Fig. 7). It records a trend broadly comparable to that of GHU *P–T* path, suggesting probably analogous fast exhumation. This trend could be explained by considering that both units are the lowest units of the Alpine tectonic pile laid directly above the Hercynian Domain. On the contrary, SCU (Cima Pedani area) and PPU (Corte area) occupy the uppermost positions in the tectonic stack of the Lower Units. Despite the different *P–T* estimates registered during the D1 phase, both units show comparable *P–T* paths. The progressive warming from the P_{peak} to the T_{peak} suggests that these units, during their exhumation, experienced progressive heating due to the re-equilibration of the isothermic field. This implies that, during their exhumation in the D1 phase, and differently from what described for GHU and CPU, SCU and PPU stationed for some time between 45 and 17 km and between 35 and 17 km, respectively. During the D2 phase, the *P–T* trends of SCU and PPU are comparable with that of CPU, although with higher *P–T* values.

CAU and PEU from the Cima Pedani area show D1-related trends similar to those of the overlying SCU and to the equivalent PPU from the Corte area, except for the relative low-*P* conditions of the *P*-peak registered in CAU, which causes the almost isobaric heating between the P_{peak} and the T_{peak}. Similarly to what was described above for SCU and PPU, the temperature is of 430 °C in CAU and PEU at the end of the D1 phase. However, the transition from the D1 to the D2 phase in these units is characterized by an almost isobaric cooling, which implies the re-cooling of CAU. A similar path during the cooling phase has been described in other orogens as related to the thrusting of initially warmer over cooler material (Chamberlain and Karabinos, 1987; Wakabayashi, 2004). Although the base of CAU is unknown, we can therefore postulate that CAU was juxtaposed over cooler units. A first possibility is that CAU overthrusts directly onto the Hercynian Corsica Domain: in this case, the observed temperature gap would be justified by the fact that CAU is in contact with a portion of the European margin that never underwent subduction. Alternatively, we could postulate an overthrusting of CAU over other, unexposed Lower Units. If so, we could argue, similarly to the scenario depicted for CPU in the Corte area, that these units experienced a much faster exhumation than CAU, because of their westernmost position (i.e. closer to the Hercynian Corsica Domain) in the unit pile.

5.3. The final stage of exhumation of the Lower Units: the D3 east-verging deformation

In the three selected areas, the D3 phase is represented by gently inclined F3 folds characterized by eastward or southeastward vergence. The crystallization of only calcite associated with the S3 axial plane foliation indicates their development at a depth of at most 10 km.

Contrary to the orientation of the S3 foliation, the trend of the A3 axes varies in the three areas, from NNE–SSW in the Corte and Ghisoni areas to ENE–WSW in the Cima Pedani area. The simplest explanation is that the changing in the orientation of the A3 axes documented in Cima Pedani area is the result of a passive rotation around a vertical axis during the sinistral strike-slip tectonics of the CCSZ.

The D3 extensional top-to-the-east shear zone has been described in the rest of Alpine Corsica and dated back to the Oligocene (Brunet et al., 2000) or to the late Oligocene–early Miocene (e.g., Malasoma et al., 2006). In line with these authors, we interpret the D3 phase as produced during an extensional tectonics, mostly developed as a consequence of the Adria slab roll-back (Gueydan et al., 2017).

Considering the differences within the *P* and *T* estimates obtained for the D1–D2 phases in GHU and in the Lower Units exposed in the Corte and Cima Pedani areas (Di Rosa et al., 2017a), and that the tectonic contacts between the Lower Units and the "Schistes lustrés" Complex were folded during the D3 event, it is supposed that the stack in southwestern Alpine Corsica occurred during the late D2 phase.

6. Conclusions

This study provides stratigraphic and tectono-metamorphic constraints to depict the involvement of the European continental crust in the processes of subduction and exhumation during the Alpine orogeny in Corsica. The data collected in the Lower Units of the Alpine tectonic prism from the Cima Pedani, Corte and Ghisoni areas indicate that:

1) according to the stratigraphy of the Lower Units, from the Triassic to the late Eocene, the sedimentation above the European continental margin evolved from shallow to pelagic marine. Starting from the Eocene, the deposition of breccias and sandstones is controlled by the erosion of the bulge, formed immediately before the subduction of the continental crust;

2) the Lower Units preserved only the retrograde migration path within the orogenic wedge;

3) *P–T* estimates indicate that each unit has an independent exhumation trajectory with different exhumation rates a function of their position within the orogenic wedge;

4) the exhumation processes started during convergence-related processes (D1 and D2 phase) and continue during extensional tectonics (D3 phase) driven by both the overthickening of the orogenic wedge and the Adria slab roll-back.

Acknowledgements

We would like to thank Jaques Malavieille and André Michard for their constructive reviews. We are also thankful to Olivier Vidal, Valentina Batanova and Valérie Magnin (IsTerre, Grenoble) for the EPMA analysis, the Italian societies SIMP, SGI, SOGEI and AIV as well as the University of Pisa (PRA project) for the financial support provided to this project.

Appendix A. Supplementary data

Supplementary data to this article can be found online at https://doi.org/10.1016/j.crte.2018.12.002.

References

Amaudric du Chaffaut, S., Caron, J.-M., Jauzein, A., Bonin, B., Rossi, P., Conchon, C., Perthuisot, J.-P., 1983. Carte géologique de la France (1/50000), feuille Venaco (111a). BRGM, Orléans, France.

Best, M.G., 2003. Igneous and Metamorphic Petrology, second ed. Brigham Young University, Blackwell Publishing. 758 p.

Bezert, P., Caby, R., 1988. Sur l'âge post-bartonien des événements tectonométamorphiques alpins en bordure orientale de la Corse cristalline (Nord de Corte). Bull. Soc. geol. France 4 (6), 965–971.

Brunet, C., Monié, P., Jolivet, L., Cadet, J.-P., 2000. Migration of compression and extension in the Tyrrhenian Sea, insights from $^{40}Ar/^{39}Ar$ ages on micas along a transect from Corsica to Tuscany. Tectonophysics 321, 127–155.

Cavazza, W., Zattin, M., Ventura, B., Zuffa, G.G., 2001. Apatite fission track analysis of Neogene exhumation in northern Corsica (France). Terra. Nova 13, 51–57.

Cavazza, W., DeCelles, P.G., Fellin, M.G., Paganelli, L., 2007. The Miocene Saint-Florent Basin in northern Corsica stratigraphy, sedimentology and tectonic implications. Basin Res. 19, 507–527.

Chamberlain, C.P., Karabinos, P., 1987. Influence of deformation on pressure-temperature paths of metamorphism. Geology 15, 42–44.

Danisik, M., Kuhlemann, J., Dunkl, I., Székely, B., Frisch, W., 2007. Burial and exhumation of Corsica (France) in the light of fission track data. Tectonics 26, TC1001.

Di Rosa, M., De Giorgi, A., Marroni, M., Vidal, O., 2017a. Syn-convergence exhumation of continental crust: evidence from structural and metamorphic analysis of the Monte Cecu area, Alpine Corsica (Northern Corsica, France). Geol. J. 52, 919–937.

Di Rosa, M., De Giorgi, A., Marroni, M., Pandolfi, L., 2017b. Geology of the area between Golo and Tavignano Valleys (Central Corsica): a snapshot of the continental metamorphic units of Alpine Corsica. J. Maps 13, 644–653.

Durand-Delga, M., 1984. Principaux traits de la Corse Alpine et corrélations avec les Alpes Ligures. Mem. Soc. Geol. It. 28, 285–329.

Faure, M., Malavieille, J., 1981. Étude structurale d'un cisaillement ductile: le charriage ophiolitique corse dans la région de Bastia. Bull. Soc. geol. France 23 (4), 355-343.

Ferrandini, J., Gattacceca, J., Ferrandini, M., Deino, A., Janin, M.C., 2003. Chronostratigraphie et paléomagnétisme des dépôts oligo-miocènes de Corse : implications géodynamiques pour l'ouverture du bassin liguro-provençal. Bull. Soc. geol. France 174 (4), 357–371.

Ferrill, D.A., Morris, A.P., Evans, M.A., Burkhard, M., Groshong, R.H., Onasch, C.M., 2004. Calcite twin morphology: a low-temperature deformation geothermometer. J. Struct. Geol. 26, 1521–1529.

Frizon de Lamotte, D., Raulin, C., Nouchot, N., Wrobel-Daveau, J.-C., Blanpied, C., Ringenbach, J.-C., 2011. The southernmost margin of the Tethys realm during the Mesozoic and Cenozoic: initial geometry and timing of the inversion processes. Tectonics 30, TC3002.

Garfagnoli, F., Menna, F., Pandeli, E., Principi, G., 2009. Alpine metamorphic and tectonic evolution of the Inzecca–Ghisoni area (southern Alpine Corsica, France). Geol. J. 44, 191–210.

Gueydan, F., Brun, J.-P., Phillippon, M., Noury, M., 2017. Sequential extension as a record of Corsica rotation during Apennines slab roll-back. Tectonophysics. https://doi.org/10.1016/j.tecto.2016.12.028.

Guillot, S., Hattori, K., Agard, P., Schwartz, S., Vidal, O., 2009. Exhumation processes in oceanic and continental subduction Contexts: a review. In: Lallemand, S., Funiciello, F. (Eds.), Subduction Zone Geodynamics. Springer-Verlag Berlin, pp. 175–205.

Lacombe, O., Jolivet, L., 2005. Structural and kinematic relationships between Corsica and the Pyrenees-Provence domain at the time of the Pyrenean orogeny. Tectonics 24, TC1003. https://doi.org/10.1029/2004TC001673.

Lanari, P., Vidal, O., De Andrade, V., Dubacq, B., Lewin, E., Grosch, E., Schwartz, S., 2014. XMAPTOOLS: a MATLAB c -based program for electron microprobe X-ray image processing and geothermobarometry. Comput. Geosci. 62, 227–240.

Maggi, M., Rossetti, F., Ranalli, G., Theye, T., 2014. Feedback between fluid infiltration and rheology along a regioonal ductile-to-brittle shear zone the East Tenda Shear Zone (Alpine Corsica). Tectonics 33, 253–280.

Malasoma, A., Marroni, M., Musumeci, G., Pandolfi, L., 2006. High pressure mineral assemblage in granitic rocks from continental units, Alpine Corsica. France. Geol. J. 41, 49–59.

Malasoma, A., Marroni, M., 2007. HP/LT metamorphism in the Volparone Breccia (Northern Corsica, France): evidence for involvement of the Europe/Corsica continental margin in the Alpine subduction zone. J. Metamorph. Geol. 25, 529–545.

Malavieille, J., Chemenda, A., Larroque, C., 1998. Evolutionary model for the Alpine Corsica: mechanism for ophiolite emplacement and exhumation of high-pressure rocks. Terra. Nova 10, 317–322.

Maluski, H., Mattauer, M., Matte, P.H., 1973. Sur la présence de décrochement alpins en Corse. C. R. Acad. Sci. Paris, Ser. II 276, 709–712.

Marroni, M., Pandolfi, L., 2007. The architecture of an incipient oceanic basin: a tentative reconstruction of the Jurassic Liguria–Piemonte basin along the Northern Apennine–Alpine Corsica transect. Int. J. Earth Sci. 96, 1059–1078.

Marroni, M., Pandolfi, L., Meneghini, F., 2004. From accretion to exhumation in a fossil accretionary wedge: a case history from Gottero Unit (Northern Apennines, Italy). Geodin. Acta 17, 41–53.

Marroni, M., Meneghini, F., Pandolfi, L., 2017. A revised subduction inception model to explain the Late Cretaceous, double vergent orogen in the pre-collisional Western Tethys: evidence from the Northern Apennines. Tectonics. https://doi.org/10.1002/2017TC004627.

Mattauer, M., Faure, M., Malaviaille, J., 1981. Transverse lineation and large-scale structures related to Alpine obduction in Corsica. J. Struct. Geol. 3 (4), 401–409.

Matte, P., 2001. The Variscan collage and orogeny (480-290 Ma) and tectonic definition of the America microplate: a review. Terra. Nova 13, 122–128.

Michard, A., Martinotti, G., 2002. The Eocene unconformity of the Briançonnais domain in the French-Italian Alps, revisited (Marguareis massif, Cuneo); a hint for a Late Cretaceous-middle Eocene frontal bulge setting. Geodin. Acta 15, 289–301.

Molli, G., Tribuzio, R., Marquer, D., 2006. Deformation and metamorphism at the eastern border of Tenda Massif (NE Corsica): a record of subduction and exhumation of continental crust. J. Struct. Geol. 28, 1748–1766.

Molli, G., Malavieille, J., 2011. Orogenic processes and the Corsica/Apennines geodynamic evolution: insights from Taiwan. Int. J. Earth Sci. 100, 1207–1224.

Pandolfi, L., Marroni, M., Malasoma, A., 2016. Stratigraphic and structural features of the Bas-Ostriconi Unit (Corsica): paleogeographic implications. C. R. Geoscuence 348, 630–640.

Passchier, C.W., Trouw, R.A.J., 2005. Microtectonics, vol. 16. Springer, Berlin, New York, 366 p.

Puccinelli, A., Perilli, N., Cascella, A., 2012. Stratigraphy of the Caporalino–Sant'Angelo Unit: a face Jurassic-Eocene succession of the alpine Corsica. Riv. Ital. Paleontol. Stratigr. 118 (3), 471–491.

Rossetti, F., Glodny, J., Theye, T., Maggi, M., 2015. Pressure-temperature-deformation-time of the ductile Alpine shearing in Corsica from orogenic construction to collapse. Lithos 218–219, 99–116.

Rossi, P., Durand-Delga, M., Caron, J.-M., Guieu, G., Conchon, O., Libourel, G., Loye-Pilot, M., 1994. Carte géologique de la France (1/50,000), feuille Corte (1110). BRGM, Orléans, France.

Rossi, P., Oggiano, G., Cocherie, A., 2009. A restored section of the "southern Variscan realm" the Corsica–Sardinia microcontinent. C. R. Geoscience 341, 224–238.

Rossi, P., Lahondère, J.-C., Cocherie, A., Caballero, Y., Feraud, J., 2012. Carte géologique de la France (1/50,000), feuille Bastelica (1118). BRGM, Orléans, France.

Saccani, E., Dilek, Y., Marroni, M., Pandolfi, L., 2015. Continental margin ophiolites of Neotethys: remnants of Ancient Ocean-Continent Transition Zone (OCTZ) lithosphere and their geochemistry, mantle sources and melt evolution patterns. Episodes 38 (4), 230–249. https://doi.org/10.18814/epiiugs/2015/v38i4/82418.

Vidal, O., Parra, T., 2000. Exhumation paths of high-pressure metapelites obtained from local equilibria for chlorite–phengite assemblage. Geol. J. 35, 139–161.

Vidal, O., Parra, T., Trotet, F., 2001. A thermodynamic model for Fe-Mg aluminous chlorite using data from phase equilibrium experiments and natural pelitic assemblages in the 100–600 °C, 1–25 kbar *P–T* range. Am. J. Sci. 301, 557–592.

Vitale Brovarone, A., Herwartz, D., 2013. Timing of HP metamorphism in the Schistes Lustrés of Alpine Corsica: new Lu–Hf garnet and lawsonite ages. Lithos 172–173, 175–191.

Wakabayashi, J., 2004. Tectonic mechanisms associated with *P–T* paths of regional metamorphism: alternatives to single-cycle thrusting and heating. Tectonophysics 392, 193–218.

Waters, C.N., 1990. The Cenozoic tectonic evolution of Alpine Corsica. J. Geol. Soc. London 147, 811–824.